DOI: 10.1002/ejic.201001154

Synthesis, Structure, and Photochemistry of an Organic Heptamolybdate-Monomolybdate

Adam Wutkowski,[a] Bikshandarkoil R. Srinivasan,*[b] Ashish R. Naik,[b] Christian Schütt,[a] Christian Näther,[a] and Wolfgang Bensch*[a]

Keywords: Photochemistry / Polyoxometalates / Molybdenum / Reduction

Treatment of MoO_3 with butan-1-amine ($BuNH_2$) or pyrrolidine ($PyrNH_2$) results in the formation of $(BuNH_3)_8[(Mo_7O_{24})(MoO_4)]\cdot 3H_2O$ (**1**; $BuNH_3$ = butan-1-aminium) or $(PyrNH_2)_6[(Mo_7O_{24}]\cdot 2H_2O$ (**2**; $PyrNH_2$ = pyrrolidinium), respectively. On irradiation with sunlight, compound **1**, which is an organic heptamolybdate $[Mo_7O_{24}]^{6-}$ that contains a cocrystallized monomolybdate $[MoO_4]^{2-}$ in the same compound, is transformed to an oxido-bridged diheptamolybdate $(BuNH_3)_{10}[(Mo_7O_{22})(\mu_2\text{-}O)_2(Mo_7O_{22})]\cdot 5.5H_2O$ (**1b**). The $[Mo_7O_{24}]^{6-}$ units in **1** and **2** are made up of edge-sharing $[MoO_6]$ octahedra, whereas the central unit in **1b** is a bis(μ_2-O)-bridged heptamolybdate dimer. Hydrogen bonding among the lattice water molecules in **1** results in the formation of a water octamer, whereas hydrogen bonding between the lattice water molecules and $[Mo_7O_{24}]^{6-}$ in **2** results in the formation of a one-dimensional water-linked heptamolybdate chain. Supramolecular structures, photochemistry, and thermal properties of **1**, **1b**, and **2** are reported. For comparison of photochemical behavior, two more polyoxomolybdates, $(PrNH_3)_6[Mo_7O_{24}]\cdot 3H_2O$ (**3**; $PrNH_3$ = propan-1-aminium) and $(PentNH_3)_6[Mo_7O_{24}]\cdot 3H_2O$ (**4**; $PentNH_3$ = pentan-1-aminium), were prepared and characterized.

Introduction

An extensive chemistry of polyoxometalates (POMs) has been developed in the last three decades,[1] and this field continues to remain a frontier area of research. Current interest in POMs and the intense research investigations over the past years can be nicely summarized by quoting the following statement from a very early review article[2] by Pope and Müller, two of the pioneering workers in this field: "Polyoxometalates form a unique class of compounds that is unmatched in terms of molecular and electronic structural versatility, reactivity and relevance in analytical chemistry, catalysis, biology, medicine, geochemistry, materials science and topology." The remarkable progress in this area can be attributed to the synthesis of several new POMs under ambient[3] and hydrothermal conditions,[4] and their structural characterization. Of the POMs of the early transition metals, Mo occupies a unique position. Several high-nuclearity polyoxomolybdate compounds that contain as many as 368 Mo atoms, which exhibit fascinating structures like giant wheels, wheels linked to chains, giant molecular spheres of the Keplerate type, giant molecular baskets, and the proteinlike nano-hedgehog, and so on, have been structurally characterized. In most Mo-based POMs, an MoO_6 octahedron is one of the building blocks for many high-nuclearity polyoxomolybdates.

Generally, polyoxomolybdates are prepared either by acidification of an alkaline tetraoxidomolybdate solution in the presence of appropriate countercations or from a neutralized molybdenum trioxide solution. The pH-dependent synthesis can be summarized as shown below.

$$[MoO_4]^{2-} \rightarrow POM \rightarrow MoO_3$$

Acidification of an aqueous alkaline solution of $[MoO_4]^{2-}$ leads to the condensation of monomeric tetrahedral $\{MoO_4\}$ units and the formation of higher-nuclearity polyoxomolybdates. The ultimate product of acidification is MoO_3, although the first product of the acidification reaction is $[Mo_7O_{24}]^{6-}$, the structure of which is made up of edge-sharing $\{MoO_6\}$ octahedra. Its formation can be written as shown in Equation (1).

$$7[MoO_4]^{2-} + 8H^+ \rightarrow [Mo_7O_{24}]^{6-} + 4H_2O \quad (1)$$

In addition to $[Mo_7O_{24}]^{6-}$, other low-nuclearity polyoxomolybdates that contain 6 and 8 Mo atoms, namely, hexa- and octamolybdates, are of considerable interest in view of their photochemical properties.[5] Unlike the all-sulfur analogue of heptamolybdate, which does not exist,[6] several heptamolybdates that are charge balanced by both inorganic and organic counterions have been synthesized and structurally characterized.[7,8] A survey of the literature reveals a rich structural chemistry of $[Mo_7O_{24}]^{6-}$ (Table 1) and a flexibility that enables it to exist in different environ-

[a] Institut für Anorganische Chemie, Christian-Albrechts-Universität Kiel
Max-Eyth Strasse 2, 24118 Kiel, Germany
E-mail: wbensch@ac.uni-kiel.de
[b] Department of Chemistry, Goa University,
Goa 403206, India
E-mail: srini@unigoa.ac.in

Supporting information for this article is available on the WWW under http://dx.doi.org/10.1002/ejic.201001154.

Table 1. Synthesis and structural features of heptamolybdates.[a]

	Compound	Space group	Mo source / acid (pH)	Ref.
1	$Na(NH_4)[bppH_2]_2[Mo_7O_{24}]\cdot 8H_2O$	$P2_1/m$	$(NH_4)_6[Mo_7O_{24}]$ / H_2SO_4 / (5.8) hydrothermal	[7a]
2	$(2\text{-apH})_6[Mo_7O_{24}]\cdot 3H_2O$	$P2_1/n$	$(NH_4)_6[Mo_7O_{24}]$ (6.0) hydrothermal	[7b] see also [7c,7d]
3	$(2\text{-apH})_4[Co(H_2O)_5Mo_7O_{24}]\cdot 9H_2O$	$Pna2_1$	$(NH_4)_6[Mo_7O_{24}]$ (6.0 to 6.3) hydrothermal	[7e]
4	$(ImH)_4[Ca(H_2O)_6(\mu\text{-}O)_2][Mo_7O_{24}]\cdot 2(Im)\cdot 3H_2O$	$C2/m$	MoO_3 / H_2SO_4 / (5.8)	[7f]
5	$(H_2DABCO)_3[Mo_7O_{24}]\cdot 4H_2O$	Cc	$(NH_4)_6[Mo_7O_{24}]$ / HCl (6)	[7g]
6	$(BuNH_3)_8[(Mo_7O_{24})(MoO_4)]\cdot 3H_2O$ (**1**)	$P\bar{1}$	MoO_3	this work
7	$(BuNH_3)_6[Mo_7O_{24}]\cdot 3H_2O$[b]	$P2_1/n$	MoO_3 (6–7)	[7h]
8	$(PyrNH_2)_6[(Mo_7O_{24}]\cdot 2H_2O$ (**2**)	$P\bar{1}$	MoO_3	this work
9	$(PrNH_3)_6[Mo_7O_{24}]\cdot 3H_2O$ (**3**)	$P\bar{1}$	$(NH_4)_6[Mo_7O_{24}]$	[7i], this work
10	$(i\text{PrNH}_3)_6[Mo_7O_{24}]\cdot 3H_2O$	$P2/n$	$(NH_4)_6[Mo_7O_{24}]$	[7i]
11	$Na_7[Mo_7O_{24}](OH)\cdot 21H_2O$	$P2/n$	Na_2MoO_4 / HCl (6.9)	[7j]
12	$(PentNH_3)_6[Mo_7O_{24}]\cdot 3H_2O$ (**4**)	$P2_1/n$	MoO_3 (6–7)	[7h], this work
13	$(HexNH_3)_6[Mo_7O_{24}]\cdot 3H_2O$	$P2_1/n$	MoO_3 (6–7)	[7h]
14	$(t\text{BuNH}_3)_6[Mo_7O_{24}]\cdot 7H_2O$	$P2_1/n$	MoO_3	[7k]
15	$(TemedH_2)_3[Mo_7O_{24}]\cdot 4H_2O$	$C2/c$	MoO_3	[7l]
16	$(hmtH)_2[\{Zn(H_2O)_5\}\{Zn(H_2O)_4\}\{Mo_7O_{24}\}]\cdot 2H_2O$	$C2/c$	Na_2MoO_4 / HCl (3)	[7m]
17	$(GuaNH_2)_6[Mo_7O_{24}]\cdot H_2O$	$C2/c$	$Na_6[Mo_7O_{24}]$	[7n]
18	$(GuaNH_2)_6[Mo_7O_{24}]\cdot H_2O$	$P2_1/c$	Na_2MoO_4	[7o]
19	$(GuaNH_2)_7Na[CoMo_7O_{24}(H_2O)_5]_2\cdot 8H_2O$	$P2_1/c$	Na_2MoO_4 / HCl (5.0)	[7p]
20	$(4\text{-apH})_6[Mo_7O_{24}]\cdot 6H_2O$	$P2_1/c$	MoO_3	[7q]
21	$[UreaH]_3(NH_4)_9[Mo_7O_{24}]_2\cdot 5[Urea]\cdot 4H_2O$	$Fddd$	MoO_3 (6.5)	[7f]
22	$(dienH_3)_2[Mo_7O_{24}]\cdot 4H_2O$	$C2/c$	MoO_3 (7.7)	[7r]
23	$(dienH_3)_2[Mo_7O_{24}]\cdot 4H_2O$	$P2_1/a$	MoO_3 (6.8)	[7r]
24	$Na_2(hmtH_2)_2[Mo_7O_{24}]\cdot 9H_2O$	$Pnma$	MoO_3	[7s]
25	$(NH_4)_6[Mo_7O_{24}]\cdot 4H_2O$	$P2_1/c$	commercial $(NH_4)_6[Mo_7O_{24}]$	[7t]
26	$Na_6[Mo_7O_{24}]\cdot 14H_2O$	$P2_1ab$	Na_2MoO_4 / $HClO_4$	[7u]
27	$NaCs_5[Mo_7O_{24}]_5\cdot H_2O$	$P\bar{1}$	MoO_3	[7v]
28	$K_6[Mo_7O_{24}]\cdot 4H_2O$	$P2_1/c$	MoO_3 / KOH (6.0)	[7t]
29	$Cs_6[Mo_7O_{24}]\cdot 7H_2O$	$P\bar{1}$	Na_2MoO_4 (7.0)	[7w]
30	$(NMe_4)_2(NH_4)_8[(Mo_7O_{22})(\mu_2\text{-}O)_2(Mo_7O_{22})]\cdot 4H_2O$	$P\bar{1}$	$(NH_4)_6[Mo_7O_{24}]$ / $h\upsilon$	[8]
31	$(BuNH_3)_{10}[(Mo_7O_{22})(\mu_2\text{-}O)_2(Mo_7O_{22})]\cdot 5.5H_2O$ (**1b**)	$P2_1/n$	compound **1** / sunlight	this work

[a] Abbreviations used: bpp = 1,3-bis(4-pyridyl)propane; 2-ap = 2-aminopyridine; Im = imidazole; DABCO = 1,4-diazabicyclo[2.2.2]-octane; $BuNH_2$ = butan-1-amine; $PyrNH_2$ = pyrrolidinium; $PrNH_2$ = propan-1-amine; $i\text{PrNH}_2$ = isopropylamine; $PentNH_2$ = pentan-1-amine; $HexNH_2$ = hexan-1-amine; $t\text{BuNH}_2$ = *tert*-butylamine; Temed = *N*,*N*,*N*,-tetramethylethylenediamine; hmt = hexamethylenetetramine; $GuaNH_2$ = guanidinium; 4-ap = 4-aminopyridine; $t\text{BuNH}_2$ = *tert*-butylamine; dien = diethylentriamine. [b] Unit-cell data from X-ray powder data.

ments. Although several organic heptamolybdates have been reported, many are based on heterocyclic amines like 1,3-bis(4-pyridyl)propane, 2-aminopyridine, imidazole, 4-aminopyridine, hexamethylenetetramine, and so on. A systematic study of the alklylammonium heptamolybdates has not been developed except the early work of Yamase[7i] and Roman et al.[7h] In our ongoing research program, we have employed organic amines as structure-directing agents and have developed a very rich structural chemistry of organic tetrasulfidomolybdates $[MoS_4]^{2-}$ and the corresponding tetrasulfidotungstates $[WS_4]^{2-}$.[9] In addition to a general base-promoted cation-exchange reaction for the facile synthesis of group VI tetrasulfidometalates that contain organic ammonium cations, we have shown that the reaction of MoO_3 with aqueous alkylamine followed by treatment with H_2S gas can be employed for the synthesis of organic $[MoS_4]^{2-}$ compounds.[9a–9g]

During the course of our study of alkylammonium tetrasulfidomolybdates,[9a–9d] we investigated the reactions of MoO_3 with several organic amines. An attempted synthesis of $(BuNH_3)_2[MoO_4]$ by treatment of MoO_3 with an excess amount of butan-1-amine ($BuNH_2$) resulted in the unexpected formation of a new organic monomolybdate that contained a cocrystallized heptamolybdate in the same compound, namely, $(BuNH_3)_8[(Mo_7O_{24})(MoO_4)]\cdot 3H_2O$ (**1**). We noted that compound **1**, upon irradiation with sunlight, developed a blue color (Figure S1 in the Supporting Information). In view of this, the neutralization reaction of MoO_3 was studied in this work under similar reaction conditions but using different organic monoamines (Scheme 1),

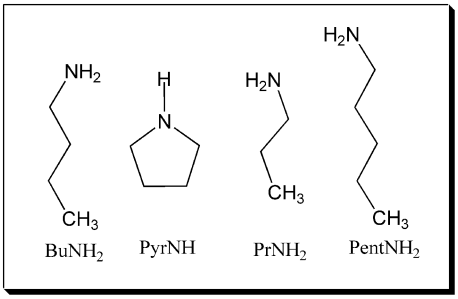

Scheme 1. Amines used in this study.

namely, propan-1-amine ($PrNH_2$), butan-1-amine ($BuNH_2$), pentan-1-amine ($PentNH_2$), and the cyclic amine pyrrolidine (PyrNH). Unlike $BuNH_2$, reactions of MoO_3 with other amines resulted in the formation of heptamolybdate products $(PyrNH_2)_6[(Mo_7O_{24}]\cdot 2H_2O$ ($PyrNH_2$ = pyrrolidinium) (**2**), $(PrNH_3)_6[Mo_7O_{24}]\cdot 3H_2O$ (**3**), ($PrNH_3$ = propan-1-aminium), and $(PentNH_3)_6[Mo_7O_{24}]\cdot 3H_2O$ (**4**) ($PentNH_3$ = pentan-1-aminium). The results of these investigations are described herein.

Results and Discussion

Description of Crystal Structures of 1, 2, and 1b

Compound **1** crystallizes in the space group $P\bar{1}$ with all atoms situated in general positions. It is unique because it is an organic heptamolybdate $[Mo_7O_{24}]^{6-}$ that also contains a cocrystallized monomolybdate $[MoO_4]^{2-}$. The structure consists of two unique $[MoO_4]^{2-}$ anions, two crystallographically independent $[Mo_7O_{24}]^{6-}$ anions, six H_2O molecules, and sixteen butan-1-aminium cations (Figure 1). In the tetrahedral $[MoO_4]^{2-}$ ions, the geometric parameters (Table S1 in the Supporting Information) are consistent with reported data.[10] Both crystallographically independent $[Mo_7O_{24}]^{6-}$ cluster anions have identical structural features and contain a central $\{Mo_3O_8\}$ core composed of three edge-sharing MoO_6 octahedra arranged in a 1×3 rectangular array; two MoO_6 units from above and two from below share the equatorial O atoms at the apices of the octahedra in the rectangle (details of the structure are in the Supporting Information). The geometrical parameters of the $[Mo_7O_{24}]^{6-}$ units (Table S1) agree well with reported values.[7] Bond-valence sum calculations yield average values for all Mo atoms close to 6.0.[11]

The organic cations, anions, and H_2O in **1** are involved in three varieties of hydrogen bonds, namely, O–H···O, N–H···O, and C–H···O. The $[MoO_4]^{2-}$ ions are hydrogen-bonded to organic cations through N–H···O interactions (Figure S2 in the Supporting Information). The lattice water molecules O83, O84, O85, and O86 (Table 2) form a centrosymmetric water octamer built by bridging two water molecules to the chair form of a cyclic water hexamer (Figure S3 in the Supporting Information). A similar water octamer was reported earlier.[12] The octamer is further hydrogen-bonded through O–H···O interactions to four symmetry-related $[Mo_7O_{24}]^{6-}$ anions that function as hydrogen acceptors (Figure 1). The two lattice water molecules O81 and O82 differ from the water octamer in that they are also hydrogen-bonded to one organic cation in addition to heptamolybdate (Figure S4 in the Supporting Information).

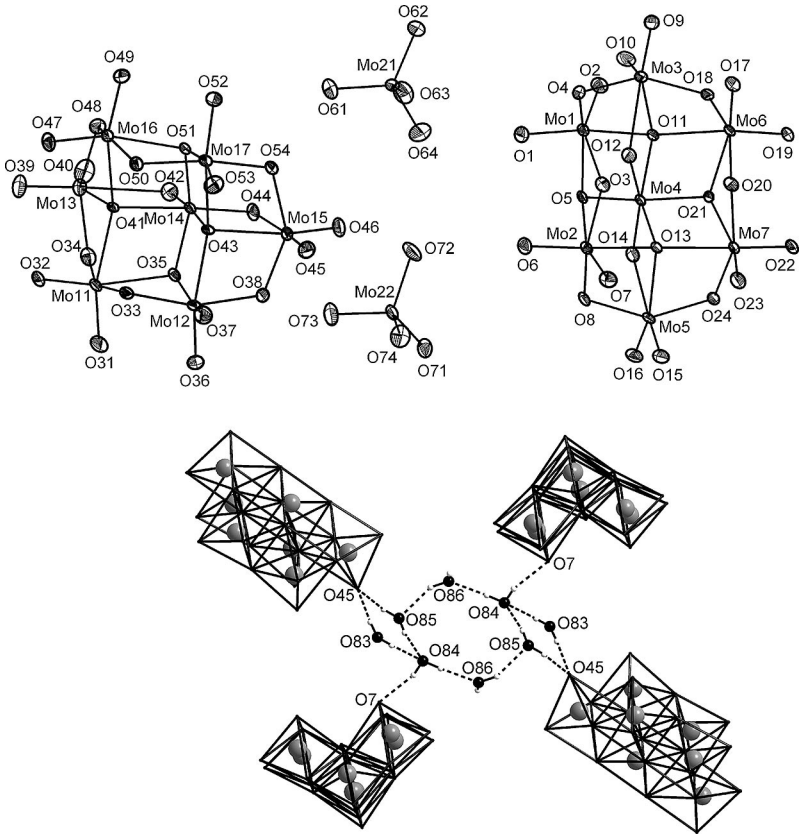

Figure 1. (Top) Crystal structure and atom labeling for compound **1** showing two unique $[MoO_4]^{2-}$ anions together with two independent $[Mo_7O_{24}]^{6-}$ anions. Displacement ellipsoids are drawn at 50% probability. H_2O molecules and butan-1-aminium cations are not shown for clarity. Bottom: A view of the centrosymmetric water octamer showing its linking to four different $[Mo_7O_{24}]^{6-}$ anions (open polyhedra), that function as hydrogen acceptors.

The pronounced disorder of six organic cations prevents a detailed description of the hydrogen-bonding situation, and relevant hydrogen-bonding interactions are given in the Supporting Information.

Table 2. Selected hydrogen-bonding parameters [Å, °] for lattice water molecules in **1** and **2**.

D–H···A	*d*(D–H)	*d*(H···A)	*d*(D···A)	< DHA	Symmetry code
$(BuNH_3)_8[(Mo_7O_{24})(MoO_4)]\cdot 3H_2O$ (**1**)					
O83–H50···O84	0.860	1.929	2.788	177	–*x*, –*y* + 1, –*z* + 1
O83–H60···O45	0.860	2.029	2.883	171	
O84–H70···O7	0.860	1.997	2.801	155	
O84–H80···O86	0.860	1.896	2.733	164	
O85–H90···O86	0.860	2.035	2.847	157	
O85–H100···O84	0.860	2.010	2.860	169	–*x*, –*y* + 1, –*z* + 1
O86–H110···O8	0.860	1.968	2.765	153	
O81–H10···O18	0.860	2.098	2.925	161	–*x*, –*y* + 2, –*z*
O81–H20···O9	0.860	2.052	2.890	164	
O82–H40···O37	0.860	2.149	2.807	138	
$(PyrNH_2)_6[Mo_7O_{24}]\cdot 2H_2O$ (**2**)					
O25–H1O···O11	0.820	1.959	2.736	157	
O25–H2O···O9	0.820	1.954	2.771	174	–*x* + 1, –*y*, –*z* + 1
O26–H3O···O15	0.820	2.148	2.890	150	–*x* + 1, –*y*, –*z* + 2
O26–H4O···O8	0.820	1.994	2.782	160	
C41–H41B···O26	0.970	2.623	3.329	130	*x* – 1, *y*, *z*
N1–H2N1···O25	0.900	1.968	2.837	161	
N5–H1N5···O26	0.900	1.932	2.780	156	–*x* + 1, –*y*, –*z* + 2

Compound **2** crystallizes in the triclinic space group $P\bar{1}$ with all atoms located in general positions. The crystal structure consists of an independent $[Mo_7O_{24}]^{6-}$ unit, six pyrrolidinium cations, and two crystal water molecules (Figure S5 in the Supporting Information). Compound **2** differs from **1** in that the monomeric $[MoO_4]^{2-}$ unit is not present. The structural and geometric features of the $[Mo_7O_{24}]^{6-}$ anion are similar to that described for the cluster anion in **1** (Table S1). Bond-valence sum calculations[11] give average values for all Mo atoms close to 6.0.

As in compound **1**, the constituents are involved in three varieties of hydrogen bonds (i.e., O–H···O, N–H···O, and C–H···O). The water molecules O25 and O26 in **2** act as hydrogen donors and hydrogen acceptors and exhibit all three kinds of hydrogen bonds (Figure S6 in the Supporting Information). One H_2O molecule (O25) is linked to two $[Mo_7O_{24}]^{6-}$ anions through two O–H···O bonds and to an organic cation through an N–H···O interaction, whereas the second water molecule (O26) is hydrogen-bonded to two heptamolybdates through two O–H···O bonds and to two organic cations with the aid of an N–H···O and C–H···O interaction, respectively. The result of the O–H···O interactions between the $[Mo_7O_{24}]^{6-}$ anions and the H_2O molecules is the formation of a one-dimensional chain along the *c* axis, on which H_2O and $[Mo_7O_{24}]^{6-}$ molecules alternate (Figure 2). Each unique heptamolybdate anion is hydrogen-bonded to four symmetry-related water molecules.

The one-dimensional chain is interconnected into a 3D network due to hydrogen bonding between cations and heptamolybdate units (geometric parameters are listed in the Supporting Information).

The blue compound **1b** crystallizes in the $P2_1/n$ space group with all atoms situated in general positions. The crystal structure consists of a crystallographically independent bis(μ_2-O)-bridged heptamolybdate dimer $[(Mo_7O_{22})(\mu_2\text{-}O)_2(Mo_7O_{22})]^{10-}$ (Figure 3), ten butan-1-aminium cations, and six H_2O molecules. Compound **1b** is structurally similar to the earlier reported mixed cationic compound $(NMe_4)_2(NH_4)_8[(Mo_7O_{22})(\mu_2\text{-}O)_2(Mo_7O_{22})]$ (NMe_4 = tetramethylammonium).[8] The central unit of **1b** is made up of two heptamolybdate fragments bridged by a pair of μ_2-O atoms (O19 and O22), which are shared by both heptamolybdate units. The two electrons introduced due to the photoreduction are delocalized over the four Mo sites Mo6,

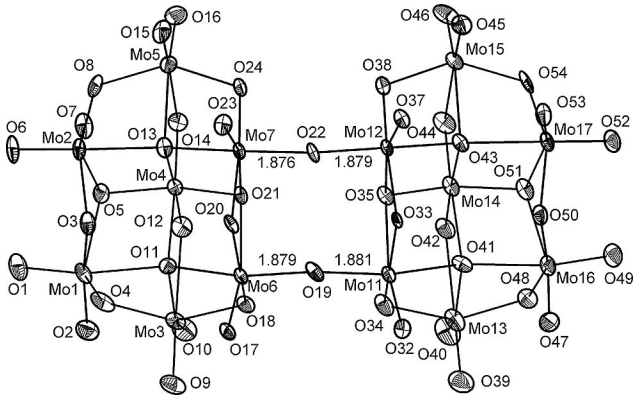

Figure 3. Crystal structure of $(BuNH_3)_{10}[(Mo_7O_{22})(\mu_2\text{-}O)_2(Mo_7O_{22})]\cdot 5.5H_2O$ **1b** showing the atom-labeling scheme. Displacement ellipsoids are drawn at 50% probability. For clarity, lattice water molecules and butan-1-aminium cations are not shown.

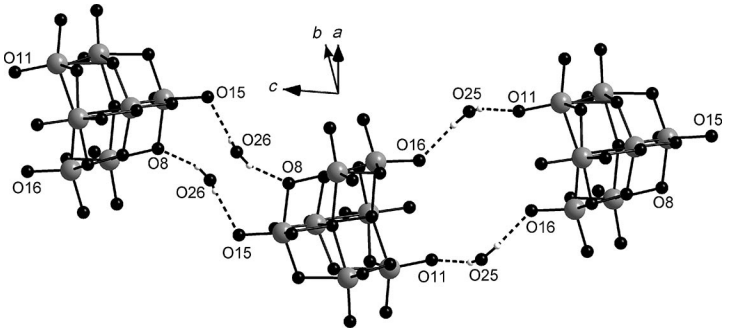

Figure 2. O–H···O interactions between the heptamolybdate and the lattice water molecules in $(PyrNH_2)_6[Mo_7O_{24}]\cdot 2H_2O$ (**2**) result in the formation of a one dimensional water-linked heptamolybdate chain that extends along the *c* axis.

Mo7, Mo11, and Mo12. The geometric parameters and structural features (details in the Supporting Information) are in excellent agreement with reported data.[8] As in compounds **1** and **2**, several weak interactions that involve the anion, lattice water molecules, and the organic cations were observed in **1b**.

Comparative Structural Features of Heptamolybdates

The structural characterization of heptamolybdates charge-balanced by a large variety of cations and metal complex cations as in $(2\text{-apH})_4[Co(H_2O)_5Mo_7O_{24}]\cdot 9H_2O$[7e] (for explanation of abbreviations, see Table 1) demonstrate the flexibility of heptamolybdate to exist in different structural environments. All heptamolybdates are hydrated and contain at least one H_2O molecule. The compounds that contain the triprotonated dien and monocationic guanidinium $(dienH_3)_2[Mo_7O_{24}]\cdot 4H_2O$ and $(GuaNH_2)_6[Mo_7O_{24}]\cdot H_2O$ exhibit polymorphism. The polymorphic modifications of $(dienH_3)_2[Mo_7O_{24}]\cdot 4H_2O$ are isolated under different reaction conditions (pH). In the case of $(GuaNH_2)_6[Mo_7O_{24}]\cdot H_2O$, the room-temperature structure data revealed a *C*2/*c* phase, whereas at 173 K the modification crystallized in $P2_1/c$. In the NH_4^+, Na^+, K^+, and Cs^+ heptamolybdates, the cations are coordinated both to O atoms of $[Mo_7O_{24}]^{6-}$ and O atoms of H_2O. Coordination of O atoms of $[Mo_7O_{24}]^{6-}$ is also observed in a few compounds like $(2\text{-apH})_4[Co(H_2O)_5Mo_7O_{24}]\cdot 9H_2O$, $(hmtH)_2[\{Zn(H_2O)_5\}\{Zn(H_2O)_4\}\{Mo_7O_{24}\}]\cdot 2H_2O$, $(GuaNH_2)_7Na[CoMo_7O_{24}(H_2O)_5]_2\cdot 8H_2O$, and $(ImH)_4[Ca(H_2O)_6(\mu\text{-}O)_2][Mo_7O_{24}]\cdot 2(Im)\cdot 3H_2O$. However, in compounds that contain only organic ammonium cations as in **1**, **2**, and so on, $[Mo_7O_{24}]^{6-}$ is involved in secondary interactions like N–H···O or C–H···O with the organic cation, and O–H···O interactions with lattice water. Of these, the O–H···O interactions are very important in view of the observation of the presence of cocrystallized water molecules in all known heptamolybdates. The heptamolybdate–water interactions can lead to interesting water architectures such as the water octamer in **1** or the one-dimensional infinite chain in **2**.

Synthetic Aspects, Spectral and Thermal Studies

Although a few of the known organic heptamolybdates (Table 1, entries–3) have been isolated under hydrothermal conditions,[7a,7b,7e] the majority were prepared under ambient conditions. In general, heptamolybdates are synthesized by dissolution of MoO_3 in an organic base or by treating ammonium heptamolybdate with an organic amine (Table 1), thereby resulting in cation exchange. In some cases, $Na_2[MoO_4]$ is used as an Mo source in acid medium in the presence of the organic cation. In aqueous solution, several Mo^{VI} species such as $[MoO_4]^{2-}$, $[Mo_{10}O_{35}]^{10-}$, $[Mo_7O_{24}]^{6-}$, $[HMo_7O_{24}]^{5-}$, $[H_3Mo_8O_{28}]^{5-}$, $[Mo_8O_{26}]^{4-}$, and so on exist in equilibrium, and the concentration of each species is pH-dependent.[13] At highly alkaline pH, $[MoO_4]^{2-}$ is the most abundant species,[10] whereas in neutral to moderately acidic solution $[Mo_7O_{24}]^{6-}$ dominates and reaches its maximum concentration at a pH of around 5.6.[13] The formation of specific polyoxometalate products depends on factors like concentration of Mo^{VI}, pH, countercation, and so on. In view of this, most of the known heptamolybdates are isolated from acidic media, although a few examples (Table 1, entries 22 or 11) have been isolated from a weakly alkaline or a nearly neutral solution, respectively.

In the present work, we have investigated the room-temperature reactions of MoO_3 with selected organic amines. The reaction of MoO_3 with aqueous $BuNH_2$ (Scheme 2) gives a clear solution (pH ≈ 11.4).

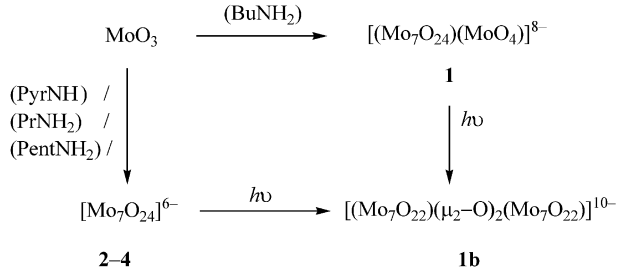

Scheme 2. Synthesis of **1**–**4** and **1b**.

Slow evaporation resulted in the formation of **1**, and the pH of the reaction mixture when crystals started forming was around 8. The crystalline product was found to be different in terms of analytical data, and the powder pattern did not match with that of $(BuNH_3)_6[(Mo_7O_{24})]\cdot 3H_2O$, which was prepared by treating MoO_3 with $H_2O/BuNH_2$ under reflux[7h] followed by crystallization in the pH range of 6–7. The structural investigation of **1** reveals the presence of both $[MoO_4]^{2-}$ and $[Mo_7O_{24}]^{6-}$ in **1**. The high formation tendency of **1** can also be evidenced by its facile formation when the same reaction is performed by using $(NH_4)_6[Mo_7O_{24}]$ instead of MoO_3. The formation of such a mixed mono-hepta system can be attributed to the different reaction conditions employed in this work. Interestingly, the treatment of MoO_3 with $PrNH_2$ or $PentNH_2$ under identical conditions did not result in the formation of a mixed mono-hepta product but $(PrNH_3)_6[(Mo_7O_{24})]\cdot 3H_2O$ (**3**) and $(PentNH_3)_6[(Mo_7O_{24})]\cdot 3H_2O$ (**4**) (Scheme 2). The synthesis of **3** and **4** have been reported earlier; it involved reacting $(NH_4)_6[Mo_7O_{24}]$ with $PrNH_2$[7i] (Table 1, entry 9) and MoO_3 heated at reflux with aqueous $PentNH_2$[7h] (Table 1, entry 12). The analytical and spectroscopic data demonstrate that **3** and **4** are identical to the earlier reported compounds. Since use of amines that contain three carbon atoms ($PrNH_2$) and five carbon atoms ($PentNH_2$) did not give a mono-hepta product, the reaction of MoO_3 was investigated using pyrrolidine (PyrNH). In this case, the isolated product turned out to be a simple heptamolybdate **2**. All attempts to prepare the reported heptamolybdate $(BuNH_3)_6[(Mo_7O_{24})]\cdot 3H_2O$ using the published procedure[7h] as well as changing pH and reaction conditions have not been successful so far. For the reported compound $(BuNH_3)_6[(Mo_7O_{24})]\cdot 3H_2O$ characterized by analyti-

cal, spectral, and thermal data, the unit cell was determined, but no atomic coordinates were reported.

Irradiation of a saturated solution of **1** with sunlight for approximately 30 min resulted in the formation of an intense blue solution from which blue crystals of **1b** were isolated. The present method of synthesis of the reduced dimeric heptamolybdate **1b** is milder and differs from the reported procedure of Yamase,[8] which involves irradiation of $(NH_4)_6[Mo_7O_{24}]$ using a 100 W mercury lamp for 20 h.

The solution and solid-state UV/Vis spectra of the colorless compounds **1** to **4** are nearly identical and exhibit a strong and broad signal centered around 208 nm (Figure S7 in the Supporting Information). The solid-state IR spectra of **1** to **4** show several signals in the mid-IR region. A common feature of all IR spectra is the appearance of a broad and strong absorption band in the O–H region around 3500 cm^{-1} due to the O–H stretching vibration of lattice water. The signals in the mid-IR range can be attributed to vibrations of the organic cations. The intense signal at around 3000 cm^{-1} is due to the υ_{N-H} vibration of the protonated amine. It is interesting to note that the IR spectra of the new compounds **1** and **2** are nearly similar (Figure S8 in the Supporting Information). The symmetric stretching vibration υ_1 of the MoO_6 unit is observed as an intense band in the Raman spectrum at around 935 cm^{-1} in **1**–**4**, respectively,[14] whereas the doubly degenerate asymmetric stretching mode υ_2 is located at 873 and 840 cm^{-1} (for **1**) and 877 and 857 cm^{-1} (for **2**). The intense doublet at around 660 and 630 cm^{-1} observed in all compounds can be assigned for the υ_{as} (Mo–O–Mo) vibration.[15]

The thermal behavior of **1** and **2**, which decompose in three steps, is nearly similar [differential thermal analysis and thermogravimetric analysis (DTA-TG) curves, Figure S9 in the Supporting Information]. In the mass spectra recorded simultaneously during decomposition, fragments of the amine molecules could be identified in the first two steps along with some unidentified signals that indicate a complex decomposition process. The observed total weight loss in both cases is more than that expected for the loss of organic amines and H_2O. The X-ray powder patterns of the residues for **1** and **2** indicate the formation of MoO_2, and in the case of **2**, additional unidentified reflections were seen. Elemental analysis of the residue revealed no residual C or N in **1**, whereas a trace amount of N (0.9%) was observed in the residue for **2**.

Photochemical Investigations

The photochemistry of organic heptamolybdates and the mechanism of photoreduction that resulted in Mo^{5+}-containing products are well documented in the literature.[5,7g,7l] It has been reported that irradiation of an aqueous solution of $(NH_4)_6[Mo_7O_{24}]$ for 20 h results in the formation of an intense blue solution[8] from which blue dimeric mixed cationic $(NMe_4)_2(NH_4)_8[(Mo_7O_{22})(\mu_2\text{-}O)_2(Mo_7O_{22})]\cdot 4H_2O$ was isolated. Prolonged UV photolysis of aqueous heptamolybdate at pH 3.9–4.1 leads to the formation of $\{Mo_{132}\}$ Keplerate species through a Mo blue intermediate.[5b] The photochemical products of compounds **1**–**4** obtained upon irradiation with UV light (310 nm) at room temperature were investigated by UV/Vis spectra. It is interesting to note that the UV/Vis spectra of the irradiation products of all compounds **1**–**4** are identical with absorption maxima at 613 and 732 nm (Figure S10 in the Supporting Information), thereby indicating the formation of the same product in all cases, which is consistent with reported data.[8,5e,5f] The photochemical reaction of the mono-hepta compound **1** requires UV-light (310 nm) irradiation for around 5 min to develop an intense blue color, whereas compounds **2**–**4** showed color change only after prolonged irradiation. The facile formation of the reduced blue species upon irradiation of the hepta-mono compound **1** can be evidenced by a comparison of the UV/Vis spectra of irradiated solutions of compounds **1**, **3**, and **4** (Figure 4) recorded after 15 min of irradiation. The spectra clearly show that formation of the reduced blue species is fastest for **1** compared to the other compounds.

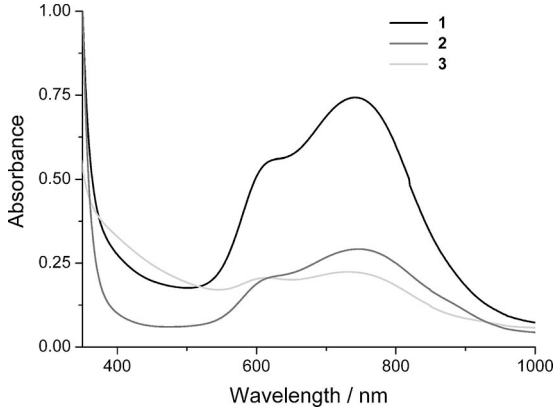

Figure 4. UV/Vis spectra of the photoreduced products of **1**, **2**, and **3** measured after irradiation for 15 min.

The above finding is consistent with our observation that an intense blue solution could be obtained by solar irradiation of **1** within a short time, whereas color change of solutions of **2**–**4** in sunlight required a longer duration. Compound **1**, which undergoes facile photoreduction, is a mono-hepta system unlike the others, which are pure heptamolybdates. Furthermore, all the compounds differ in terms of the organic cation. It is to be noted that the photoreduced blue species undergo slow reoxidation in all cases with time and become colorless (for time-resolved UV/Vis spectra, see Figure S10 in the Supporting Information). To understand the differing photochemical behavior of the mono-hepta compound **1** compared to those of pure heptamolybdates, the role of the charge-balancing organic cations and the influence of the residual gas in irradiated solutions were investigated by time-dependent photochemical experiments.

The reoxidation behavior of compound **1** strongly depends on the actual condition of the solution (Figure 5). The fastest reoxidation was observed by applying an O_2

stream during the irradiation experiments (series a). Even after 6 irradiation cycles, decoloration was achieved after about 40 min, which is roughly two times longer than for the first irradiation. The results obtained with series c (control) show a different slope and a prolonged time for reoxidation. The longest time for decoloration was observed for series b (Ar-saturated solution), which was more than four times longer than for the solution with oxygen. Note that the same trends were observed for compounds **2**–**4**.

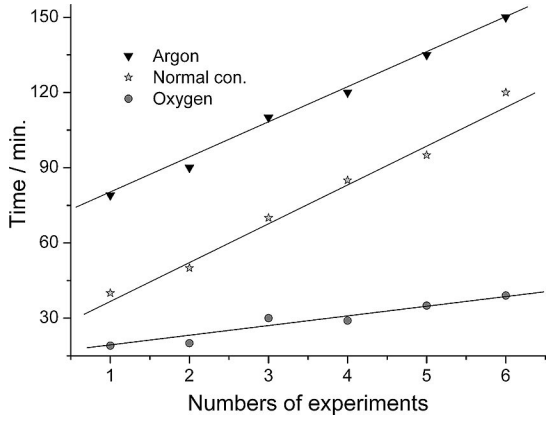

Figure 5. Reoxidation time of compound **1** as function of irradiation cycles and the gas in the solution. Lines are guides for the eyes.

A comparison of the photochemical behavior in the presence of an O_2 stream of all four compounds is shown in Figure 6. The shortest time for reoxidation was observed for **1**, whereas **2** needed roughly 20 times longer for decolorization. Compounds **3** and **4** behave similarly, with a slightly shorter time period for full reoxidation for **3**. The main difference between these two compounds are the ammonium cations R–NH_3 with R = *n*-propyl for **3** and R = *n*-pentyl for **4**. Note that both ammonium cations contain alkyl chains, whereas in compound **2** charge compensation is achieved by the pyrrolidinium cation. It has been reported that monomethyl- and monoethylammonium polyoxomolybdate salts could not be reoxidized,[5] and secondary ammonium salts of polyoxomolybdates are photochromic.[16]

Our present results clearly demonstrate the influence of the gaseous species present in the solutions and are in accordance with the reported mechanism of photoreduction.[5a,5e,5f] The fastest reoxidation occured by bubbling O_2 through the solution, and the reaction was hindered when Ar was bubbled through the solution. In addition, the reoxidation time was prolonged by increasing the irradiation cycle due to the consumption of the organic cation. Further experiments were conducted to determine the role of O_2 and of the amine. Compound **1** was dissolved in air-free distilled water purged with a stream of Ar gas. Dissolution of **1** was done with an Ar stream bubbling through water, and then the vial was tightly sealed. The solution was irradiated until an intense blue color appeared, and this solution was kept in the dark for several weeks; it exhibited no optical change of the color over this long time period. This observation can be regarded as conclusive evidence that molecular O_2 is required for the decoloration (i.e., for the reoxidation). Investigation of the role of the amine was done in the following way. A solution of **1** was irradiated several times, thereby leading to a reoxidation time of about 50 min. Then butylamine (30 μL) was added to the colorless solution (T = 21.3 °C, final pH = 11.6), and this mixture was irradiated again. But no blue color appeared, even after long irradiation times. When the pH value of this solution was adjusted to 4.9 (T = 21.3 °C), irradiation immediately colorized the solution. Clearly, the whole system is sensitive to the pH value, which may be explained on the basis of the pH-dependent equilibrium of dissolved molybdate species. A similar observation was made for solutions of **2** and **3**, for which no color change could be observed if the pH value was higher than 6.3 (see Figure 7). A possible explanation of the dependency on the pH value can be that at under more acidic conditions the amount of protonated amines is larger, thus leading to the formation of more CT complexes and increasing the reoxidation time. For pH >

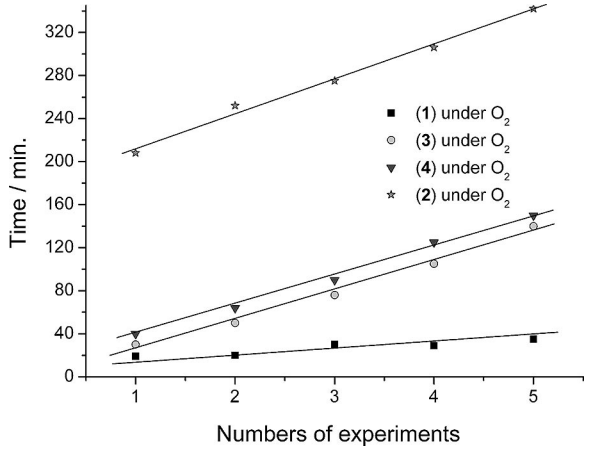

Figure 6. Comparison of reoxidation behavior of the four compounds as function of irradiation cycles. During the experiments oxygen was bubbled through the solution.

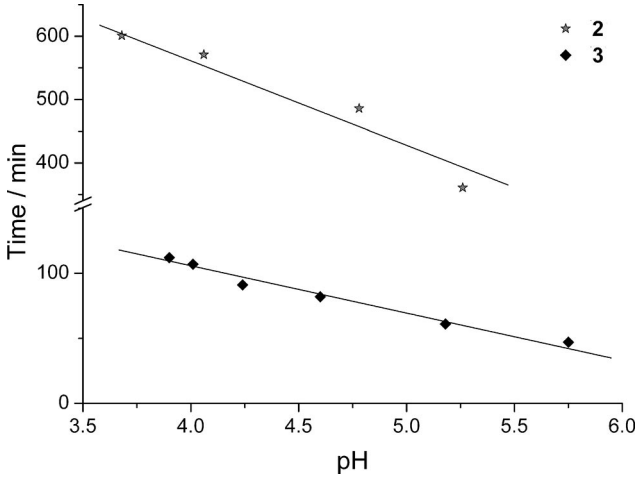

Figure 7. Comparison of reoxidation behavior of compound **2** and **3** as a function of pH.

6.3, the concentration of the heptamolybdate complex is very small because the equilibrium shifts toward isolated $[MoO_4]$ tetrahedra in the solution.

To determine whether the colored species in solution consists of the dimeric or monomeric polyoxomolybdate ions, ESI-MS experiments (masses *m*/*z* up to 3000) were undertaken with a solution of compound **2** in the oxidized and reduced state. The spectra are complex due to the large number of Mo isotopes and the gas-phase reactions that occurred in the MS apparatus. No mass signal could be identified that accounted for dimeric species.

It has been reported[5a] that the distance N···O between the N atom of the cation and the O atom of the MoO_6 octahedron determines the stability of the colored state, with optimal N···O separations between about 2.8 and 3.2 Å. In compounds **1** to **4**, the N···O separations are very similar (i.e., the formation of the CT complex is not sterically hindered by the pyrrolidine in **2** or the aliphatic chains in **3** and **4**). It is more likely that the number of C atoms and the type of the N atoms determines the reoxidation behavior. Compounds **3** and **4** contain aliphatic ammonium cations with different chain lengths, and it seems that the amine with the larger number of C atoms forms a more stable charge-transfer complex (i.e., reoxidation needs more time). On the other hand, compound **1**, which contains the $[MoO_4]^{2-}$ as well as the heptamolybdate anion, is most sensitive against irradiation and is reoxidized much faster than the other compounds. This indicates that the $[MoO_4]^{2-}$ present in **1** is responsible for this different behavior. A series of experiments was carried out by adding the appropriate amount of Na_2MoO_4 to solutions of **2** to **4** to yield a 1:1 hepta/mono ratio. The pH values of the solutions increased very slightly. The reoxidation time after UV-light irradiation remained the same within 1 or 2 min. In addition, the pH value of the $[MoO_4]^{2-}$-containing solutions was adjusted with HCl to the pH values of the original solutions, thus leading to a prolongation of the reoxidation time of about 5 min.

Conclusion

In this work, we have described the synthesis, structural characterization, and photochemical properties of a unique organic heptamolybdate that contains a cocrystallized monomolybdate $(BuNH_3)_8[(Mo_7O_{24})(MoO_4)]\cdot 3H_2O$ (**1**) and a new organic heptamolybdate $(C_4H_{10}N)_6[(Mo_7O_{24}]\cdot 2H_2O$ (**2**) charge-balanced by pyrrolidinium cations. Solar irradiation or UV photolysis of **1** results in the formation of the dimeric oxido-bridged compound $(BuNH_3)_{10}[(Mo_7O_{22})(\mu_2\text{-}O)_2(Mo_7O_{22})]\cdot 5.5H_2O$ (**1b**). Time-dependent photochemical experiments under different atmospheres show that the photochemical redox processes are influenced by the charge-balancing organic cations and the residual gas in irradiated solutions. Photochemical studies reveal that the mono-hetpa compound **1** undergoes faster photoreduction than simple organic heptamolybdates. The nearly same photochemical behavior of pure organic heptamolybdates **2** to **4** and solutions of **2** to **4**, which contained externally added $[MoO_4]^{2-}$ such that the hepta/mono ratio is 1:1, clearly indicate the unique nature of compound **1**. The facile formation of the blue heptamolybdate dimer **1b** upon solar irradiation of the hepta-mono compound **1** within a shorter time duration, unlike the earlier reported[8] extensive photolysis (20 h) required for the formation of the same blue heptamolybdate dimeric core, indicates that the dimeric core is the primary condensation product during the photochemical reduction of heptamolybdates under weakly acidic conditions. This result assumes importance in view of a recent study[5b] that reports the prolonged UV photolysis of aqueous heptamolybdate at pH 3.9 to 4.1, which leads to the formation of $\{Mo_{132}\}$ Keplerate through the Mo blue intermediate. Current efforts in our laboratories are directed towards understanding the exact role of the isolated tetrahedral $[MoO_4]^{2-}$ units in photochemical redox processes and to characterize new condensation products of the hepta-mono compound **1** at different pH values.

Experimental Section

Materials and Methods: All the chemicals and solvents were used in this investigation as obtained from commercial sources with analytical purity. Far-IR spectra (range 80 to 500 cm^{-1}) were recorded with a Bruker IFS 66 infrared spectrometer. Mid-IR spectra were recorded in a KBr matrix with a Shimadzu (IR Prestige-21) FTIR spectrometer and an ATI Mattson Genesis infrared spectrometer in the range 4000–400 cm^{-1}. Raman spectra were recorded in the region 100 to 3500 cm^{-1} with a Bruker FRA 106 Fourier transform Raman spectrometer. The homogeneity of the different compounds was examined with X-ray powder diffractometry (STOE STADI-P, λ = 1.54056 Å). TG-DTA measurements were performed under a nitrogen atmosphere in Al_2O_3 crucibles with a STA-409CD simultaneous thermal analyzer from Netzsch. A heating rate of 4 K min^{-1} was employed for all measurements. Solid-state and solution electronic spectra of the samples were recorded in transmittance mode with a Cary 5000 instrument from Varian. For solid-state spectra, the samples were diluted with KBr, and KBr was used as reference, whereas for solution spectra an aqueous solution (3 mL of 0.0265 mmol of **1**, **2**, **3**, and **4**; pH of **1** = 5.10, **2** = 4.97, **3** = 5.25, **4** = 5.51) of the sample and water (reference) were taken in a pair of matched quartz cells.

Investigation of Optical Properties: Time-dependent optical properties of the compounds were investigated by taking samples (0.0265 mmol) in deionized water (3 mL) in quartz tubes. For preliminary experiments and recording of UV/Vis spectra, solutions of compounds **1**, **2**, **3**, and **4** were irradiated with UV light of wavelength 310 nm with a lamp from Apex Illuminators M-66450, Newport. For all photochemical investigations, solutions of samples **1** to **4** were irradiated with a UV-P250c lamp (Panacol–Elsol) that supplied continuous light in the range of 200 to 600 nm. The quartz tubes were placed at a distance of 15 cm from the lamp and irradiated for 5 min, and later the samples were stored in the dark until full decoloration was reached. The irradiation and decoloration procedure was performed six times for every sample.

Investigation of the Influence of Oxygen (Series a): A constant stream of oxygen (75 mL min^{-1}) was bubbled through the solutions during irradiation. The solutions were then stored in dark under oxygen stream.

Table 3. Selected details of data acquisition and refinement of compounds **1**, **1b**, and **2**.

	1	**1b**	**2**
Crystal system	triclinic	monoclinic	triclinic
Space group	$P\bar{1}$	$P2_1/n$	$P\bar{1}$
a [Å]	18.9667(14)	17.7321(16)	11.1794(7)
b [Å]	19.4915(14)	25.8797(17)	11.4767(8)
c [Å]	20.7979(14)	21.6971(17)	20.5740(13)
α [°]	68.831(8)	90.0	82.314(8)
β [°]	67.851(8)	111.263(10)	78.0190(8)
γ [°]	80.811(9)	90.0	64.6930(7)
V [Å^3]	6638.4(8)	9279.0(13)	2331.4(3)
Z	4	4	2
$D_{calcd.}$ [g cm^{-3}]	1.864	2.090	2.172
μ [mm^{-1}]	1.542	1.914	1. 911
Scan range	$2.22 \leq 2\theta \leq 28.03$	$1.87 \leq 2\theta \leq 24.01$	$2.26 \leq 2\theta \leq 28.02$
Reflections collected	64976	37605	22828
Independent reflections	31132 [R(int) = 0.0645]	14121 [R(int) = 0.0661]	10944 [R(int) = 0.0364]
GOF on F^2	0.961	1.048	0.952
Final R indices	$R1$ = 0.0414	$R1$ = 0.0541	$R1$ = 0.0352
[$I > 2\sigma(I)$]	$wR2$ = 0.1009	$wR2$ = 0.1257	$wR2$ = 0.0837
R indices (all data)	$R1$ = 0.0577, $wR2$ = 0.1076	$R1$ = 0.0743, $wR2$ = 0.1338	$R1$ = 0.0499, $wR2$ = 0.0891
Largest diff peak and hole [e Å^{-3}]	1.167 / –1.860	2.183 / –2.112	1.542 / –1.219

Investigation of the Influence of Argon (Series b): The solution was saturated with Ar by bubbling a stream of Ar through the solution (75 mL min^{-1}) for 5 min. Afterwards the glass tube was sealed and irradiated by applying the procedure described above. After full decoloration, the same sample was used for subsequent irradiation experiments without further Ar purging. Control experiments (series c) were done without purging the solutions with a gas flow and by applying the same conditions presented above.

Synthesis of 1–4: Molybdic acid (3.24 g) was added to water (5 mL) to obtain a slurry. $BuNH_2$ (5 mL) was added, and the almost-clear solution was filtered and left aside for crystallization. After a week, crystals were observed. At the point of crystallization, the pH was around 8.06. The crystals were isolated by filtration and dried in air to afford $(BuNH_3)_8[(Mo_7O_{24})(MoO_4)]\cdot 3H_2O$ (**1**). Use of PyrNH (5 mL)/$PrNH_2$ (5 mL)/$PentNH_2$ (5 mL) instead of $BuNH_2$ in the above reaction under identical conditions resulted in the formation of $(PyrNH_2)_6[Mo_7O_{24}]\cdot 2H_2O$ (**2**) or $(PrNH_3)_6[Mo_7O_{24}]\cdot 3H_2O$ (**3**) or $(PentNH_3)_6[Mo_7O_{24}]\cdot 3H_2O$ (**4**). Anal. calcd. for $C_{32}H_{102}Mo_8N_8O_{31}$ (**1**): C 20.63, H 5.52, N 6.02; found C 20.81, H 5.62, N 6.15. IR (KBr): $\tilde{\nu}$ = 3435, 2961, 2932, 2865, 2767, 2526, 2056, 1615, 1511, 1465, 1382, 1332, 1170, 1078, 1037, 873, 840, 782, 661, 628, 576, 481, 398, 367 cm^{-1}. Raman: $\tilde{\nu}$ = 2964, 2936, 2910, 2873, 1448, 1077, 1048, 936 (υ_1), 891, 630, 401, 353, 217, 117 cm^{-1}. Anal. calcd. for $C_{24}H_{58}Mo_7N_6O_{26}$ (**2**): C 18.91, H 4.23, N 5.51; found C 19.44, H 4.3, N 5.6. IR (KBr): $\tilde{\nu}$ = 3426, 3142, 2964, 2764, 2476, 1617, 1604, 1491, 1452, 1087, 947, 857, 782, 671, 617, 563, 478, 413 cm^{-1}. Raman: $\tilde{\nu}$ = 2979, 2833, 1450, 1033, 1048, 941, 932 (υ_1), 916, 891, 866, 626, 351, 215, 110 cm^{-1}. Anal. calcd. for $C_{18}N_6H_{66}Mo_7O_{27}$ (**3**): C 14.70, H 4.52, N 5.72; found C 15.05, H 4.61, N 5.9. IR (KBr): $\tilde{\nu}$ = 3441, 3103, 2967, 2935, 2865, 2531, 1605, 1503, 1485, 1387, 1211, 877, 851, 681, 668, 511 cm^{-1}. Raman: $\tilde{\nu}$ = 2964, 2935, 2874, 1449, 1330, 1052, 934 (υ_1), 888, 353, 215, 123 cm^{-1}. Anal. calcd. for $C_{30}H_{90}Mo_7N_6O_{27}$ (**4**): C 21.99, H 5.13, N 5.54; found C 22.16, H 5.59, N 5.18. IR (KBr): $\tilde{\nu}$ = 3425, 3040, 2942, 2869, 2718, 2524, 2047, 1615, 1481, 1467, 1384, 1232, 861, 839, 661, 634, 577, 503 cm^{-1}. Raman: $\tilde{\nu}$ = 2967, 2933, 2918, 2879, 1441, 1079, 1049, 934 (υ_1), 890, 635, 353, 213, 112 cm^{-1}.

Synthesis of $(BuNH_3)_{10}[(Mo_7O_{22})(\mu_2\text{-}O)_2(Mo_7O_{22})]\cdot 5.5H_2O$ (1b): For preparation of compound **1b**, **1** (1.2 g) was dissolved in water (4 mL) to get a saturated solution (pH = 6.1). Upon exposure to sunlight, the color of the reaction mixture changed to blue in about 30 min, and the blue reaction mixture was kept in the dark. A few blue crystals were isolated from the reaction mixture, and one crystal was used for structure determination.

X-ray Crystallography: Intensity data for **1**, **1b**, and **2** were collected with an Image Plate Diffraction System (IPDS-1) from STOE. The structures were solved with direct methods using SHELXS-97,[17] and refinements were carried out against F^2 by using SHELXL-97.[17] All non-hydrogen atoms were refined using anisotropic displacement parameters. The C–H hydrogen atoms were positioned with idealized geometry and refined using a riding model. Some of the organic cations in compound **1**, **1b**, and **2** were disordered and were refined using a split model. In compounds **1** and **1b**, some of the N–H and O–H hydrogen atoms could not be located and thus were not considered. The other hydrogen atoms were located in a difference map, their bond lengths set to ideal values; and finally they were refined using a riding model. Selected refinement results are given in Table 3.

Supporting Information (see footnote on the first page of this article): Detailed description of the structures, IR spectra, UV/Vis spectra of solutions of the title compounds along with crystallographic data can be found in the online version.

CCDC-805553 (for **1**), -805554 (for **2**) and -805555 (for **1b**) contain the supplementary crystallographic data for this paper. These data can be obtained free of charge from The Cambridge Crystallographic Data Centre via www.ccdc.cam.ac.uk/data_request/cif.

Acknowledgments

Financial support by the State of Schleswig-Holstein and the Fonds der Chemischen Industrie (to W. B.) and grants under the Special Assistance Programme [F.540/25/DRS/2007/(SAP-I)] of the University Grants Commission, New Delhi (to B. R. S.) is gratefully acknowledged. A. W. thanks K. and D. Wutkowski as well as H. Lühmann and J. Djamil for their support.

[1] a) M. T. Pope, A. Müller, in: *Polyoxometalates: From Platonic Solids to Anti-Retroviral Activity*, Kluwer, The Netherlands,

1994; b) M. T. Pope, A. Müller in: *Polyoxometalate Chemistry: From Topology via Self-Assembly to Applications*, Kluwer, The Netherlands, **2001**; c) M. T. Pope, in: *Hetropoly and Isopoly Oxometalates*, Springer, Berlin, **1983**; d) U. Kortz, A. Müller, J. Slageren, J. Schnack, N. S. Dalal, M. Dressel, *Coord. Chem. Rev.* **2009**, *253*, 2315–2327.

[2] M. T. Pope, A. Müller, *Angew. Chem. Int. Ed. Engl.* **1991**, *30*, 34–48.

[3] a) N. Belai, P. N. Kapoor, M. H. Dickman, R. J. Butcher, M. T. Pope, *Eur. J. Inorg. Chem.* **2009**, 5215–5218; b) R. Khoshnavazi, H. Eshtiagh-Hosseini, M. H. Alizadeh, M. T. Pope, *Inorg. Chim. Acta* **2007**, *360*, 686–690; c) C. M. Flynn Jr., M. T. Pope, *Inorg. Chem.* **1971**, *10*, 2524–2529; d) F. Hussain, U. Kortz, B. Keita, L. Nadjo, M. T. Pope, *Inorg. Chem.* **2006**, *45*, 761–766; e) K. Wassermann, M. T. Pope, *Inorg. Chem.* **2001**, *40*, 2763–2768; f) C. Rong, M. T. Pope, *J. Am. Chem. Soc.* **1992**, *114*, 2932–2938; g) M. I. Khan, S. Tabassum, C. L. Marshall, M. K. Nylon, *Catal. Lett.* **2006**, *112*, 1–12; h) A. Müller, *Chem. Commun.* **2003**, 803–806; i) A. Müller, A. M. Todea, H. Bögge, J. V. Slageren, M. Dressel, A. Stammler, M. Rusu, *Chem. Commun.* **2006**, 3066–3068; j) A. Müller, P. Kögerler, C. Kuhlmann, *Chem. Commun.* **1999**, 1347–1358; k) A. Müller, M. Koop, H. Bögge, M. Schmidtmann, C. Beugholt, *Chem. Commun.* **1998**, 1501–1502; l) A. Müller, M. Koop, H. Bögge, M. Schmidtmann, F. Peters, P. Kögerler, *Chem. Commun.* **1999**, 1885–1886; m) A. Müller, R. Sessoli, E. Krickemeyer, H. Bögge, J. Meyer, D. Gatteschi, L. Pardi, J. Westphal, K. Hovemeier, R. Rohlfing, J. Döring, F. Hellweg, C. Beugholt, M. Schmidtmann, *Inorg. Chem.* **1997**, *36*, 5239–5250; n) U. Kortz, M. G. Savelieff, B. S. Bassil, M. H. Dickman, *Angew. Chem. Int. Ed.* **2001**, *40*, 3384–3386; o) A. H. Ismail, B. S. Bassil, I. Römer, N. C. Redeker, U. Kortz, *Z. Naturforschung, Teil B* **2010**, *65*, 383–389.

[4] a) S. Jones, H. Liu, C. J. O'Connor, J. Zubieta, *Inorg. Chem. Commun.* **2010**, *13*, 412–416; b) W. Ouellette, H. Liu, K. Whitenack, C. J. O'Connor, J. Zubieta, *Cryst. Growth Des.* **2009**, *9*, 4258–4261; c) W. Ouellette, A. V. Prosvirin, J. Valeich, K. R. Dunbar, J. Zubieta, *Inorg. Chem.* **2007**, *46*, 9067–9082; d) P. DeBurgomaster, W. Ouellette, H. Liu, C. J. O'Connor, J. Zubieta, *CrystEngComm* **2010**, *12*, 446–469; e) P. DeBurgomaster, H. Liu, C. J. O'Connor, J. Zubieta, *Inorg. Chim. Acta* **2010**, *363*, 330–337; f) R. Kiebach, C. Näther, W. Bensch, *Solid State Sci.* **2006**, *8*, 964–970; g) R. Kiebach, C. Näther, P. Kögerler, W. Bensch, *Dalton Trans.* **2007**, 3221–3223; h) A. Wutkowski, C. Näther, P. Kögerler, W. Bensch, *Inorg. Chem.* **2008**, *47*, 1916–1918; i) A. Wutkowski, C. Näther, W. Bensch, *Z. Anorg. Allg. Chem.* **2009**, *635*, 753–758; j) A. Wutkowski, C. Näther, M. Speldrich, P. Kögerler, W. Bensch, *Z. Anorg. Allg. Chem.* **2009**, *635*, 1094–1099.

[5] a) T. Yamase, *Chem. Rev.* **1998**, *98*, 307–326; b) T. Yamase, S. Kumagai, P. V. Prokop, E. Ishikawa, A. Tomsa, *Inorg. Chem.* **2010**, *49*, 9426–9437; c) T. Yamase, P. Prokop, *Angew. Chem. Int. Ed.* **2002**, *37*, 466–469; d) R. Dessapt, D. Kervern, M. Bujoli-Doeuff, P. Deniard, M. Evain, S. Jobic, *Inorg. Chem.* **2010**, *49*, 11309–11316; e) T. Yamase, R. Sasaki, T. Ikawa, *J. Chem. Soc., Dalton Trans.* **1981**, 628–634; f) T. Yamase, T. Ikawa, *Bull. Chem. Soc. Jpn.* **1977**, *3*, 746–749.

[6] B. R. Srinivasan, *J. Chem. Sci.* **2004**, *116*, 251–259; B. R. Srinivasan, S. N. Dhuri, A. R. Naik, *Tetrahedron Lett.* **2004**, *45*, 2247–2249.

[7] a) X. Qu, L. Xu, Y. Yang, F. Li, W. Guo, L. Jia, X. Liu, *Struct. Chem.* **2008**, *19*, 801–805; b) K. Pavani, A. Ramanan, *Eur. J. Inorg. Chem.* **2005**, 3080–3087; c) J. M. Gutierrez-Zorrilla, P. Roman, C. Esteban-Calderon, M. Martinez-Ripoll, S. Garcia-Blanco, *Acta Crystallogr., Sect. A* **1984**, *40*, C229–231; d) P. Roman, J. M. Gutierrez-Zorrilla, M. Martinez-Ripoll, S. Garcia-Blanco, *Trans. Met. Chem.* **1986**, *11*, 143–150; e) T. Li, J. Lu, S. Gao, R. Cao, *Inorg. Chem. Commun.* **2007**, *10*, 1342–1346; f) P. Gili, P. A. Lorenzo-Luis, A. Mederos, J. M. Arrieta, G. Germain, A. Castineiras, R. Carballo, *Inorg. Chim. Acta* **1999**, *295*, 106–114; g) V. Coue, R. Dessapt, M. Bujoli-Doeuff, M. Evain, S. Jobic, *Inorg. Chem.* **2007**, *46*, 2824–2835; h) P. Roman, J. M. Gutierrez-Zorrilla, A. Luque, M. Martinez-Ripoll, *J. Crystallogr. Spectrosc. Res.* **1988**, *18*, 117–131; i) Y. Ohashi, K. Yanagi, Y. Sasada, T. Yamase, *Bull. Chem. Soc. Jpn.* **1982**, *55*, 1254–1260; j) J. Cruywagen, W. Esterhuysen, B. B. Heyns, *Inorg. Chim. Acta* **2003**, *348*, 205–211; k) P. Roman, A. San Jose, A. Luque, J. M. Gutierrez-Zorrilla, *Acta Crystallogr., Sect. C* **1994**, *50*, 1031–1034; l) J.-Y. Niu, X.-Z. You, H.-K. Fun, Z.-Y. Zhou, B.-C. Yip, *Polyhedron* **1996**, *15*, 1003–1008; m) T. Arumuganathan, A. Srinivasarao, T. V. Kumar, S. K. Das, *J. Chem. Sci.* **2008**, *120*, 95–97; n) A. Don, T. J. R. Weakley, *Acta Crystallogr., Sect. Acta Crystallogr., Sect. B* **1981**, *37*, 451–453; o) S. Reinoso, M. H. Dickman, A. Praetorius, U. Kortz, *Acta Crystallogr., Sect. E* **2008**, *64*, m614–615; p) C.-B. Li, *Acta Crystallogr., Sect. E* **2007**, *63*, m1911–1912; q) P. Roman, J. M. Gutierrez-Zorrilla, M. Martinez-Ripoll, S. Garcia-Blanco, *Z. Kristallogr.* **1985**, *173*, 283–292; r) P. Roman, A. Luque, A. Aranzabe, J. M. Gutierrez-Zorrilla, *Polyhedron* **1992**, *11*, 2027–2038; s) W.-B. Yang, C.-Z. Lu, H. H. Zhuang, *Jiegou Huaxue* **2002**, *21*, 168–173; t) H. T. Evans, B. M. Gatehouse, P. Leverett, *J. Chem. Soc., Dalton Trans.* **1975**, 505–514; u) K. Sjoebom, B. Hedman, *Acta Chem. Scand.* **1973**, *27*, 3673–3691; v) Z. I. Khazheeva, E. G. Khaikina, K. M. Khal'baeva, T. A. Shibanova, V. N. Molchanov, V. I. Simonov, *Kristallografiya* **2000**, *45*, 996–1002; Z. I. Khazheeva, E. G. Khaikina, K. M. Khal'baeva, T. A. Shibanova, V. N. Molchanov, V. I. Simonov, *Crystallogr. Rep.* **2000**, *45*, 916–918; w) U. Kortz, M. T. Pope, *Acta Crystallogr., Sect. C* **1995**, *51*, 1717–1719.

[8] T. Yamase, *J. Chem. Soc., Dalton Trans.* **1991**, 3055–3063.

[9] a) B. R. Srinivasan, S. V. Girkar, C. Näther, W. Bensch, *J. Coord. Chem.* **2010**, *63*, 931–942; b) B. R. Srinivasan, A. R. Naik, C. Näther, W. Bensch, *Indian J. Chem.* **2009**, *48A*, 769–774; c) B. R. Srinivasan, S. V. Girkar, C. Näther, W. Bensch, *J. Coord. Chem.* **2009**, *62*, 3559–3572; d) B. R. Srinivasan, C. Näther, A. R. Naik, W. Bensch, *Acta Crystallogr., Sect. E* **2006**, *62*, m1635–m1637; e) B. R. Srinivasan, S. N. Dhuri, C. Näther, W. Bensch, *Inorg. Chim. Acta* **2005**, *358*, 279–287; f) B. R. Srinivasan, S. N. Dhuri, C. Näther, W. Bensch, *Z. Naturforsch., Teil B* **2004**, *59*, 1083–1092; g) B. R. Srinivasan, S. N. Dhuri, A. R. Naik, C. Näther, W. Bensch, *Polyhedron* **2008**, *27*, 25–34; h) B. R. Srinivasan, S. N. Dhuri, M. Poisot, C. Näther, W. Bensch, *Z. Anorg. Allg. Chem.* **2005**, *631*, 1087–1094; i) B. R. Srinivasan, A. R. Naik, C. Näther, W. Bensch, *Z. Anorg. Allg. Chem.* **2007**, *633*, 582–588; j) B. R. Srinivasan, C. Näther, S. N. Dhuri, W. Bensch, *Monats. Chem.* **2006**, *137*, 397–411; k) B. R. Srinivasan, C. Näther, S. N. Dhuri, W. Bensch, *Polyhedron* **2006**, *25*, 3269–3277; l) B. R. Srinivasan, A. R. Naik, S. N. Dhuri, C. Näther, W. Bensch, *Polyhedron* **2009**, *28*, 3715–3722; m) B. R. Srinivasan, A. R. Naik, M. Poisot, C. Näther, W. Bensch, *Polyhedron* **2009**, *28*, 1379–1385.

[10] a) W. Bensch, P. Hug, R. Emmenegger, A. Reller, H. R. Oswald, *Mater. Res. Bull.* **1987**, *22*, 447–454; b) E. C. Alyea, G. Ferguson, Z. Xu, *Acta Crystallogr., Sect. C* **1995**, *51*, 353–356.

[11] Bond valence sums were determined using the software VaList: A. S. Wills, VaList, Program available from www.ccp14.ac.uk.

[12] T. K. Prasad, M. V. Rajasekharan, *Cryst. Growth Des.* **2006**, *6*, 488–491.

[13] J. J. Cruywagen, A. G. Draaijer, J. B. B. Heyns, E. A. Rohwer, *Inorg. Chim. Acta* **2002**, *331*, 322–329.

[14] M. Isaac, T. Pradip, V. U. Nayar, *J. Solid State Chem.* **1994**, *112*, 132–138.

[15] G. Mahata, K. Biradha, *Inorg. Chim. Acta* **2007**, *360*, 281–285.

[16] F. Arnaud-Neu, M.-J. Schwing-Weill, *Bull. Soc. Chim. Fr.* **1973**, *12*, 3225–3228.

[17] G. M. Sheldrick, *Acta Crystallogr., Sect. A* **2008**, *64*, 112–122.

Received: October 28, 2010
Published Online: April 1, 2011

